Published in final edited form as:
J Cereb Blood Flow Metab. 2009 January ; 29(1): 197–205. doi:10.1038/jcbfm.2008.112.

Magnetic Resonance Imaging Assessment of Regional Cerebral Blood Flow after Asphyxial Cardiac Arrest in Immature Rats

Mioara D. Manole, MD
Children's Hospital of Pittsburgh Department of Pediatrics Division of Pediatric Emergency Medicine

Lesley M. Foley, BSc(Hons)
Pittsburgh NMR Center for Biomedical Research Mellon Institute Carnegie Mellon University

T. Kevin Hitchens, PhD
Pittsburgh NMR Center for Biomedical Research Mellon Institute Carnegie Mellon University

Patrick M. Kochanek, MD
Children's Hospital of Pittsburgh Departments of Pediatrics and Critical Care Medicine

Robert W. Hickey, MD
Children's Hospital of Pittsburgh Department of Pediatrics Division of Pediatric Emergency Medicine

Hülya Bayir, MD
Children's Hospital of Pittsburgh Departments of Pediatrics and Critical Care Medicine Safar Center for Resuscitation Research

Henry Alexander
Safar Center for Resuscitation Research

Chien Ho, PhD
Pittsburgh NMR Center for Biomedical Research Mellon Institute Carnegie Mellon University

Robert S.B. Clark, MD
Children's Hospital of Pittsburgh Departments of Pediatrics and Critical Care Medicine

Abstract

Cerebral blood flow (CBF) alterations after asphyxial cardiac arrest (CA) are not defined in developmental animal models or humans. We characterized regional and temporal changes in CBF from 5 to 150 min after asphyxial CA of increasing duration (8.5, 9, 12 min) in postnatal day (PND) 17 rats using the noninvasive method of arterial spin-labeled magnetic resonance imaging (ASL-MRI). We also assessed blood brain barrier (BBB) permeability, and evaluated the relationship between CBF and mean arterial pressure after resuscitation. After all durations of asphyxia CBF alterations were region-dependent. After 8.5 and 9 min asphyxia, intense subcortical hyperemia at 5 min was followed by return of CBF to baseline values by 10 minutes. After 12 min asphyxia, hyperemia was absent and hypoperfusion reached a nadir of 38-65% of baselines with the lowest values in the cortex. BBB was impermeable to gadoteridol 150 min after CA. CBF in the 12 min CA group was blood pressure passive at 60 min assessed via infusion of epinephrine. ASL-MRI assessment of CBF after asphyxial CA in PND 17 rats reveals marked duration and region-specific reperfusion patterns and identifies possible new therapeutic targets.

Address for correspondence: Mioara D. Manole, MD Children's Hospital of Pittsburgh Department of Pediatrics Division of Pediatric Emergency Medicine 3705 Fifth Avenue Pittsburgh, PA 15213-2583 Phone: 412-692-7692 Fax: 412-692-7464 Email: mioara.manole@chp.edu.

Keywords

cardiac arrest; anoxia; rat; global ischemia; CBF autoregulation

Introduction

Optimal recovery of cerebral blood flow (CBF) has been implicated as a critical factor in determining neuronal survival after asphyxial cardiac arrest (CA) in infants and children. CBF after CA is well described in adult animal models; however there are limited data on CBF after pediatric asphyxial CA. In adult CA models CBF after CA is phasic in nature, with global hyperemia present for 15-30 min after return of spontaneous circulation (ROSC) characterized by CBF 2-3 times higher than baseline, followed by delayed hypoperfusion that occurs after 15-30 min and continues for several hours after ROSC (Kagstrom et al. 1983; Snyder et al. 1975).

Non-traumatic CA in pediatric victims is asphyxial in nature in a majority (90%) of cases (Young et al. 2004), and this is in contrast to predominantly ventricular fibrillation (VF) CA seen in adults. In asphyxial CA a period of systemic hypoxemia, hypercapnea, acidosis, hypotension and bradycardia precede CA (Fink et al. 2004). Few studies have characterized CBF after neonatal or pediatric global ischemia or hypoxia, and there is variability in reperfusion patterns reported: prolonged hypoxia (90 min) without CA in neonatal lambs produced hyperemia followed by hypoperfusion (Rosenberg 1986); global cerebral ischemia via cerebrospinal fluid compression in newborn piglets produced hyperemia followed by hypoperfusion in all brain regions except for cortex, where hypoperfusion was present after ROSC (Leffler et al. 1989); cerebral ischemia combined with hypoxia (Rice-Vannucci model) in postnatal day (PND) 7 rats resulted in post resuscitation CBF that was not different than baseline at 30 min, 4 and 24 hours (Mujsce et al. 1990).

Arterial spin-labeled magnetic resonance imaging (ASL-MRI) allows serial assessment of regional CBF. This technique can be applied to small rodents (Foley et al. 2005) and is ideal for application to a clinically relevant pediatric asphyxial CA model (Fink et al. 2004). Accordingly, using ASL-MRI we report serial and regional CBF changes after pediatric asphyxial CA.

Materials and methods

Studies were approved by the Institutional Animal Care and Use Committee at the University of Pittsburgh. An established pediatric asphyxial CA model developed in our center (Fink et al. 2004) was used. Mixed litter, mixed gender PND 16-18 Sprague-Dawley rats (30-45 g), n=6-7/group were used. The rats underwent the following durations of asphyxia: 8.5 min (n=7), 9 min (n=6) and 12 min (n=7). Sham control rats (n=6) underwent anesthesia and surgery without asphyxia or resuscitation. The experimental paradigm is depicted in Figure 1.

Anesthesia and surgery

The rats were initially anesthetized with 3% isoflurane/50% N_2O/balance oxygen in a Plexiglas chamber until unconscious and then the trachea was intubated with an 18-gauge angiocatheter. Mechanical ventilation was started and ventilatory rates and tidal volumes were adjusted to maintain $PaCO_2$ 35-45 mm Hg. Femoral arterial and venous catheters (PE 10) were inserted via cutdown. Mean arterial pressure (MAP) and heart rate were continuously monitored. Rectal temperature was continuously monitored and maintained at 37°C via a heated water blanket during the surgery and via a warm air heating system (SA instruments, Stony Brook, NY) during the MRI experiments. During surgery, anesthesia was obtained by ventilation with 2.5

% isoflurane/50% N2O/balance oxygen. Intravenous analgesia and paralysis were started after catheter insertion, using a fentanyl infusion at 50 μg kg^{-1} h^{-1} and vecuronium infusion 5 mg kg^{-1} h^{-1}. Fentanyl infusion dosing was based on the work of Statler et al (Statler et al. 2000). A 30 min period of isoflurane washout was performed before baseline CBF measurements to reduce the confounding effects of inhaled anesthetics on CBF (Hendrich et al. 2001). Baseline ASL-MRI were obtained. Arterial blood gas measurements were obtained at the time of arterial catheter insertion, immediately before baseline CBF measurement, after CA and at the end of the experiment and the ventilatory rates and tidal volumes were adjusted to a target of $PaCO_2$ of 35-45 mm Hg.

Asphyxial insult

A bolus of vecuronium (1mg/kg, iv) was administered 2 min before asphyxia to prevent gasping (Manole et al. 2006). The FiO_2 was reduced to 0.21 (room air) for 1 min before asphyxia to avoid hyperoxygenation. The tracheal tube was disconnected from the ventilator for 8.5, 9 or 12 min. Resuscitation was started by reconnecting the ventilator at a FiO_2 of 1.0. Epinephrine 0.005 mg/kg and sodium bicarbonate 1 mEq/kg were administered iv, followed by manual chest compressions until ROSC. After ROSC, anesthesia and neuromuscular blockade were restarted. A FiO_2 of 1.0 was maintained until 15 min after ROSC, and decreased to 0.4 for the remainder of the experiment.

Magnetic resonance image acquisition and data analysis

ASL-MRI perfusion maps were obtained at baseline and at 5, 10, 15, 30, 60, 90, 120, and 150 min after ROSC from CA. MR studies were performed on a 7-Tesla, 21-cm-bore Bruker Biospec system equipped with a 12-cm-diameter shielded gradient insert and a 72 mm volume RF coil. Data were acquired for T_2-weighted images, perfusion images (Detre et al. 1992), spin-lattice relaxation time maps of tissue water (T_1obs) (Hendrich et al. 1999), and spin-labeling efficiency measurements within the carotid arteries (Zhang et al. 1993). T_2-weighted spin-echo images were acquired with the following parameters: field of view (FOV) = 3 cm, slice thickness = 1 mm, interslice distance = 2 mm, TR/TE = 2500/40 ms, NA=2, five slices, and matrix = 128 × 70. Perfusion images were acquired using ASL (Detre et al. 1992) with continuous flow-induced adiabatic inversion for 2 s with a constant-amplitude RF pulse in the presence of a 1 G/cm field gradient along the headfoot axis of the animal. The labeling pulse for the inversion plane was positioned ± 2 cm from the perfusion detection plane. The parameters were: matrix = 64 × 40, zero-filled to 64 × 64; TR = 2000 ms; summation of three echoes; TE = 10, 20, and 30 ms; and NA=2. Spin-labeling efficiency was determined from intensities within the carotid arteries with the use of gradient-echo images (Zhang et al. 1993). Images were acquired 1 cm posterior to the plane selected for perfusion detection, with spin-labeling applied at ± 10 mm. The perfusion encoding parameters were the same as those mentioned above, and included a 45° flip angle, eight averages, TR/TE = 100/9.6 ms, and matrix = 256 × 256. The spin-lattice relaxation time of tissue water (T_1obs) (Hendrich et al. 1999) was measured from a series of spin-echo images acquired with variable TR (TR = 8000, 4300, 2300, 1200, 650, 350, 185, and 100 ms). Other parameters are as follows: TE = 9 ms, two averages, and matrix = 64 × 40. Image Analysis: All image processing was performed with the Bruker ParaVision 3.0.2 image analysis software. Regions of interest were defined in the left and right hemispheres guided by assignments from a rat brain atlas and included the cortex, hippocampus, thalamus, and amygdala/piriform cortex. Pixel-by-pixel maps of (MC - ML) • M were generated from the perfusion data (where MC is the magnetization intensity from the control image, and ML is the magnetization intensity from the labeled image). T1obs maps were generated from the series of variable TR images by a three-parameter nonlinear fit to , $M(TR) = M0 [1 - A \exp(-TR/T1obs)]$, where M(TR) is the signal intensity for each TR value, M0 is the signal intensity at equilibrium, and A is the saturation correction factor.

Regional CBF was calculated from the formula $CBF = \lambda \cdot (T1obs\ 2\alpha)^{-1} \cdot (MC — ML) \cdot MC^{-1}$ where λ is the blood-brain partition coefficient of water (Herscovitch and Raichle 1985), assuming a spatially constant value of 0.9 mL/g, and α is the spin-labeling efficiency measured in the carotids. Perfusion maps during cardiac arrest were obtained to determine the intrinsic error in the measurement of CBF in our study. For these experiments T1 obs was measured during cardiac arrest and we assume an alpha coefficient of 0.7. With the limitations of the above assumptions, CBF during cardiac arrest is 9-10 ml/100 g/min, which is within the established error range of 10 mL/100g/min for ASL as previously reported

Relationship between blood pressure and CBF

A separate group of rats (n=4) underwent 12 min of asphyxia followed by epinephrine infusion. Epinephrine was started at 1 μg/kg/min one hour after ROSC and was titrated until MAP returned to baseline. To exclude a direct effect of epinephrine-induced increases in MAP on CBF in PND 17 rats, a group of sham operated animals (n=3) were given epinephrine to increase MAP > 10 mm Hg above baseline. CBF maps pre- and post- infusion of epinephrine were compared.

Assessment of the BBB

To assess BBB permeability, we used an established technique via MRI using the paramagnetic contrast agent gadoteridol (Gd-HP-DO3A). We infused 0.2 mg/kg gadoteridol iv via the femoral catheter 150 min after ROSC. Before and 30 min after infusing gadoteridol, we obtained T_1-weighted images (TR = 600ms, TE = 15ms, FOV = 3cm, 256 × 256 matrix and NA=2). BBB permeability was assessed by subtracting pre and post infusion images. This method is sensitive to detect BBB permeability early after brain injury(Hendrich et al. 1997).

Statistical Analysis

Data were analyzed with the statistical package SPSS version 15. Data were expressed as mean ± SEM. A $p < 0.05$ was considered significant. We used one-way ANOVA with Tukey post-hoc test to compare the weight, baseline CBF, time to CA and duration of CA. We used repeated measures ANOVA to compare MAP, $PaCO_2$, PaO_2, pH, and CBF values for the four groups at each time point and to determine the differences within each group over time.

Results

Physiological data

Body weight was similar among groups. CA occurred 2.9±0.18 min after the start of asphyxia, with no difference between groups (Table 1). MAP, $PaCO_2$, PaO_2 and pH at baseline and after ROSC are shown in Table 2. Five min after ROSC, MAP was increased compared with baseline in the 8.5 min group, and was decreased compared with baseline in the 12 min group. Beyond 15 min after ROSC all three asphyxia groups had MAP values lower than baseline, with no difference between groups. $PaCO_2$ values did not differ between groups at baseline, 30 and 90 min post ROSC. $PaCO_2$ values at 150 min were lower in the 12 min group compared with 8.5 or 9 min groups. PaO_2 was lower in the 12 min group at 15 min post ROSC, and returned to baseline values afterwards. pH values were lower after ROSC in the sham groups compared with asphyxial groups and at 15 min post ROSC compared with baseline in 12 min asphyxial group.

Regional CBF after asphyxial CA

Baseline global hemispheric CBF was 198±11 ml/100g/min. Baseline CBF was heterogeneous in the five brain structures: thalamus 252±17 ml/100g/min, hippocampus 215±14 ml/100g/min, cortex 199±11 ml/100g/min, and amygdala 152±8 ml/100g/min. There were no gross

differences in CBF between male and female rats, at baseline or after CA. Figure 2 illustrates regional CBF at the 9 time points studied in one representative animal from each group.

Hemispheric CBF (Figure 3A) displayed early hyperemia in the 8.5 min asphyxia group at 5 min after ROSC (153% of baseline, $p<0.05$) and subsequently returned to baseline values for the remaining period of monitoring. In the 9 min asphyxia group hemispheric CBF displayed early hyperemia at 5 min after ROSC (143% of baseline, $p<0.05$), after which CBF decreased and was lower than baseline at 60 and 120 min after ROSC. In the 12 min asphyxia group early hyperemia was absent, and hemispheric CBF was lower than baseline after ROSC and reached a nadir of 58% baseline at 150 min.

Cortical CBF (Figure 3B) did not exhibit early hyperemia after asphyxia. Hypoperfusion was present from 10 to 150 min after ROSC in the 8.5 and 9 min asphyxia group (nadir of 63% and 52 % of baseline respectively) and 5 to 150 min after ROSC in the 12 min asphyxia group (nadir of 38% of baseline).

Thalamic CBF (Figure 3C) displayed early hyperemia in the 8.5 and 9 min asphyxia groups at 5 min after ROSC (204% and 188% of baseline, respectively, $p<0.05$), and subsequently decreased to baseline values 10 and 60 min after ROSC, respectively. In the 12 min asphyxia group initial hyperemia was not observed and thalamic CBF displayed hypoperfusion from 60 min after ROSC, reaching a nadir of 62% baseline at 150 min.

Hippocampal CBF (Figure 3D) was higher than baseline at 5 min after ROSC in the 8.5 and 9 min groups (153% and 165% of baseline respectively, $p<0.05$). CBF was not different than baseline from 10 min after ROSC. In the 12 min asphyxia group, early hyperemia was not seen, and hippocampal CBF displayed hypoperfusion 15 min after ROSC, with a nadir of 65% of baseline at 150 min.

CBF in the amygdala (Figure 3E) displayed early hyperemia in the 8.5 and 9 min groups at 5 min after ROSC (152% and 158% of baseline, $p<0.05$). CBF decreased towards baseline after 5 min and was lower than baseline in the 8.5 min group at two time points (15 and 60 min). In the 9 min group, hypoperfusion was present and persistent from 10 min after ROSC reaching a nadir of 53% of baseline at 30 min. In the 12 min group, early hyperemia was not seen, and hypoperfusion was present and persistent from 10 min, reaching a nadir of 47% of baseline at 60 min after ROSC.

Relationship between MAP and CBF

MAP was statistically significant albeit modestly decreased compared to baseline starting 15 min after ROSC in all three groups (Table 2). We assessed the response of CBF to increasing MAP in a separate group of animals undergoing 12 min asphyxia by measuring CBF 60 min after ROSC, before and after increasing MAP to baseline values via iv epinephrine infusion (dose range 5-30 μg/kg/min) (Dewachter et al. 2007). Figure 4 illustrates CBF before and after correction of MAP to baseline values in each of the four animals studied. After administration of epinephrine CBF increased compared to pre-infusion and baseline levels in all regions of interest ($p<0.01$). Thus, it appears that CBF is blood pressure passive after resuscitation from 12 min asphyxial CA. Epinephrine infusion in sham animals increased MAP by 10-25 mmHg and did not change global and regional CBF (hemispheric CBF 224±13 at baseline vs. 209±35 ml/100g/min post epinephrine), suggesting that epinephrine induced increases in MAP alone do not affect CBF in PND 17 rats not subjected to asphyxia.

Assessment of BBB permeability

At 150 min after ROSC there was no difference between the signal produced pre and post infusion of gadoteridol, indicating that there was no BBB permeability to this tracer in the four

groups of rats 150 to 180 min after asphyxial CA. Figure 5 illustrates T1 weighted images of a representative rat from each group before and 30 min after infusion of gadoteridol.

Discussion

To our knowledge this is the first study that defines serial and regional CBF after pediatric asphyxial CA in immature rats. To summarize, regional post-CA CBF ranges from hyperemia in the thalamus to hypoperfusion in the cortex and progressively longer asphyxia durations lead to prominent immediate or delayed hypoperfusion without a hyperemic phase.

Previous studies in experimental models examining reperfusion patterns after increasing durations of CA or global cerebral ischemia have produced variable results. This is likely secondary to model differences. Some studies found no difference between the magnitude of hypoperfusion with increasing duration of ischemia (Michenfelder and Milde 1990), whereas others found more intense hyperemia with short insults (Liachenko et al. 2001) or more intense hypoperfusion with longer insults (Singh et al. 1992). We demonstrated that increasing duration of CA produces a progressive reduction of perfusion at 15-30 min after resuscitation. Mechanisms that lead to postischemic hypoperfusion remain controversial. Delayed hypoperfusion may be due to impaired endothelial control of CBF (Hossmann 1997; Ten and Pinsky 2002) or to decreased metabolic demand (Michenfelder and Milde 1990). Lee et al (Lee et al. 1989) demonstrated that CBF during cardiopulmonary resuscitation (CPR) was inversely proportional to the duration of CA before CPR, ranging from 30% of baseline CBF for a 1 min CA to zero for a 9 min CA. Results of our study combined with these earlier observations of progressive decrease in CBF during CPR with longer CA durations raise the hypothesis that vascular stasis during longer CA durations leads to progressively more extensive no-reflow in a time dependent fashion. Likewise, there may be regional differences in no-reflow between brain areas; based on our data, cortical areas could have more extensive no-reflow versus other regions of the brain.

A prominent finding of our study is the absence of hyperemia and the predominance of hypoperfusion in the cortex. Most studies demonstrate early cortical hyperemia after CA (Liachenko et al. 2001; Mortberg et al. 2007). However, there was absence of hyperemia in the cortex in pig and rat global ischemia models produced by CSF compression (Kagstrom et al. 1983; Leffler et al. 1989). Likewise, in a study of short durations of asphyxia in newborn piglets, asphyxial episodes of 1 to 3 min without CA caused a 25% decrease of CBF in the cortex, whereas hippocampus, thalamus and cerebellum showed increases of CBF. Cortical hypoperfusion was postulated to be caused by sympathetic-mediated vasoconstriction (Goplerud et al. 1989). Alternatively sympathetic receptor activation may result in cortical hypoperfusion, secondary to greater density of adrenergic nerve endings in cortical vs. subcortical vessels (Edvinsson 1975; Neubauer and Edelman 1984). Other possible mechanisms mediating cortical hypoperfusion are: decreased NO production, increased superoxide production, or decreased metabolism (Liu et al. 2003; Wainwright et al. 2007).

The BBB was not permeable to the small molecule gadoteridol 3 h after resuscitation in our model. Schleien et al (Schleien et al. 1991) reported that CPR does not disrupt the BBB in adult and immature animals. BBB permeability in pigs was first noted at 4 h after VF (Schleien et al. 1991). We are unaware of any studies assessing the permeability of BBB after asphyxial CA in animals or humans.

In our model MAP was decreased after asphyxial CA vs. baseline in all groups. This is consistent with other studies where CA of significant duration was induced, and it is consistent with the clinical course of humans (Mortberg et al. 2007). We infused epinephrine to test the response to normalizing blood pressure in the 12 min asphyxia group. CBF increased to levels

above baseline, indicating that CBF after asphyxial CA of 12 min in our model is blood pressure passive. Blood pressure autoregulation of CBF after CA is impaired in comatose patients (Nishizawa and Kudoh 1996) and it is either absent or right-shifted early after CA (Sundgreen et al. 2001). In a dog model of global ischemia, blood pressure autoregulation was attenuated (Christopherson et al. 1993). We realize that we are testing blood pressure autoregulation in a setting of moderate postresuscitation hypotension. However, MAP in our animals ranged from 53% to 86% of baseline MAP and is unlikely to be below the lower limit of autoregulation.

We measured CBF with ASL-MRI because it allows serial determinations of regional CBF. This noninvasive imaging modality uses endogenous water as a freely diffusible tracer to measure CBF. It can be applied to small animals such as immature rats (Qiao et al. 2004) and provides quantitative maps of CBF. ASL-MRI has a resolution of 450 micrometers which was critical to our study. This method was used in a cardioplegic CA model in adult rats by Liachenko (Liachenko et al. 2001) and in VF CA in cats (Krep et al. 2003). To our knowledge, this is the first report of measuring CBF after CA with the ASL-MRI method in an immature animal. Our model is clinically relevant for the study of pediatric resuscitation and uses rats at PND 17, a time of active synaptogenesis, analogous to 2 to 4 year old human brain development (Harris et al. 1992). It represents the age in rats with the highest level of normal CBF (Nehlig et al. 1989).

There are challenges related to an experiment in the MRI setting on a small animal. The experimental setup includes long arterial and venous catheters and ventilator tubing that must reach equipment placed outside of the magnetic field. In a small animal, blood sampling is also limited. Some of our $PaCO_2$ values were outside of physiological range. $PaCO_2$ was significantly lower at 150 min in 12 min vs. 8.5 and 9 min groups. This raises the possibility that lower CBF in 12 min group is due to cerebral vasoconstriction in response to lower $PaCO_2$. However, there was no significant difference between $PaCO_2$ values at 90 min between the three groups, while CBF was similar at 90 min and 150 min. This argues against, but does not completely rule out an effect of $PaCO_2$ between groups. After ROSC shams had lower pH vs. the asphyxial groups, likely due to the fact that bicarbonate was not given to the shams. However, pH or CBF were not different vs. baseline in this group.

Although early hyperemia is regarded as beneficial and hypoperfusion as detrimental (Safar et al. 1996; Sterz et al. 1992), the optimal reperfusion pattern after CA is unknown (Cerchiari et al. 1987). Our results suggest important differences in reperfusion patterns with increasing duration of CA and a need for time-sensitive or CBF-directed therapeutic approach. It is not entirely known whether cerebral perfusion after ROSC is coupled to cerebral metabolism. Further studies are needed to also determine regional cerebral metabolism after ROSC from CA in our model and to determine the relevance of different levels of hyperemia and hypoperfusion to neuropathological outcome.

In conclusion, our study defines CBF after resuscitation from three increasing durations of CA in immature rats. Postresuscitation CBF is insult duration-dependent, shorter insults result in hyperemia and resolution of baseline CBF, whereas longer insults result in hypoperfusion without hyperemia. There is marked regional variability of CBF, with hypoperfusion of the cortex and hyperemia of the thalamus. Postresuscitation CBF appears blood pressure passive. Future studies are needed to define the relationship between the CBF, metabolism, histology and outcome after asphyxial CA in the developing brain.

Acknowledgements

Supported by: T32 NS07485-02 (MDM), Laerdal Foundation (MDM), RO1 HD045968 (RSBK), NS 30318 (PMK), NS 38087(PMK), P41EB-001977 (The Pittsburgh NMR Center).

References

Cerchiari EL, Hoel TM, Safar P, Sclabassi RJ. Protective effects of combined superoxide dismutase and deferoxamine on recovery of cerebral blood flow and function after cardiac arrest in dogs. Stroke 1987;18:869–878. [PubMed: 3629645]

Christopherson TJ, Milde JH, Michenfelder JD. Cerebral vascular autoregulation and CO2 reactivity following onset of the delayed postischemic hypoperfusion state in dogs. J Cereb Blood Flow Metab 1993;13:260–268. [PubMed: 8436617]

Detre JA, Leigh JS, Williams DS, Koretsky AP. Perfusion imaging. Magn Reson Med 1992;23:37–45. [PubMed: 1734182]

Dewachter P, Raeth-Fries I, Jouan-Hureaux V, Menu P, Vigneron C, Longrois D, Mertes PM. A comparison of epinephrine only, arginine vasopressin only, and epinephrine followed by arginine vasopressin on the survival rate in a rat model of anaphylactic shock. Anesthesiology 2007;106:977–983. [PubMed: 17457129]

Edvinsson L. Neurogenic mechanisms in the cerebrovascular bed. Autonomic nerves, amine receptors and their effects on cerebral blood flow. Acta Physiol Scand Suppl 1975;427:1–35. [PubMed: 56123]

Fink EL, Alexander H, Marco CD, Dixon CE, Kochanek PM, Jenkins LW, Lai Y, Donovan HA, Hickey RW, Clark RS. Experimental model of pediatric asphyxial cardiopulmonary arrest in rats. Pediatr Crit Care Med 2004;5:139–144. [PubMed: 14987343]

Foley LM, Hitchens TK, Kochanek PM, Melick JA, Jackson EK, Ho C. Murine orthostatic response during prolonged vertical studies: effect on cerebral blood flow measured by arterial spin-labeled MRI. Magn Reson Med 2005;54:798–806. [PubMed: 16142710]

Goplerud JM, Wagerle LC, Delivoria-Papadopoulos M. Regional cerebral blood flow response during and after acute asphyxia in newborn piglets. J Appl Physiol 1989;66:2827–2832. [PubMed: 2745346]

Harris KM, Jensen FE, Tsao B. Three-dimensional structure of dendritic spines and synapses in rat hippocampus (CA1) at postnatal day 15 and adult ages: implications for the maturation of synaptic physiology and long-term potentiation. J Neurosci 1992;12:2685–2705. [PubMed: 1613552]

Hendrich KS, Kochanek PM, Melick JA, Schiding JK, Statler KD, Williams DS, Marion DW, Ho C. Cerebral perfusion during anesthesia with fentanyl, isoflurane, or pentobarbital in normal rats studied by arterial spin-labeled MRI. Magn Reson Med 2001;46:202–206. [PubMed: 11443729]

Hendrich KS, Kochanek PM, Williams DS, Schiding JK, Marion DW, Ho C. Early perfusion after controlled cortical impact in rats: quantification by arterial spin-labeled MRI and the influence of spin-lattice relaxation time heterogeneity. Magn Reson Med 1999;42:673–681. [PubMed: 10502755]

Hendrich KS, Schiding JK, Kochanek P, Whalen MJ, Williams D, Ho C. Sequential MRI Assessment of Cerebral Blood Flow and Blood Brain Barrier Permeability Early After Traumatic Brain Injury in Rats. J Cereb Blood Flow Metab 1997:S76.

Herscovitch P, Raichle ME. What is the correct value for the brain--blood partition coefficient for water? J Cereb Blood Flow Metab 1985;5:65–69. [PubMed: 3871783]

HossmannKAReperfusion of the brain after global ischemia: hemodynamic disturbances. Shock1997895101; discussion 102-103 [PubMed: 9261898]

Kagstrom E, Smith ML, Siesjo BK. Local cerebral blood flow in the recovery period following complete cerebral ischemia in the rat. J Cereb Blood Flow Metab 1983;3:170–182. [PubMed: 6841464]

Krep H, Bottiger BW, Bock C, Kerskens CM, Radermacher B, Fischer M, Hoehn M, Hossmann KA. Time course of circulatory and metabolic recovery of cat brain after cardiac arrest assessed by perfusion- and diffusion-weighted imaging and MR-spectroscopy. Resuscitation 2003;58:337–348. [PubMed: 12969612]

Lee SK, Vaagenes P, Safar P, Stezoski SW, Scanlon M. Effect of cardiac arrest time on cortical cerebral blood flow during subsequent standard external cardiopulmonary resuscitation in rabbits. Resuscitation 1989;17:105–117. [PubMed: 2546227]

Leffler CW, Busija DW, Mirro R, Armstead WM, Beasley DG. Effects of ischemia on brain blood flow and oxygen consumption of newborn pigs. Am J Physiol 1989;257:H1917–1926. [PubMed: 2513731]

Liachenko S, Tang P, Hamilton RL, Xu Y. Regional dependence of cerebral reperfusion after circulatory arrest in rats. J Cereb Blood Flow Metab 2001;21:1320–1329. [PubMed: 11702047]

Liu XL, Wiklund L, Nozari A, Rubertsson S, Basu S. Differences in cerebral reperfusion and oxidative injury after cardiac arrest in pigs. Acta Anaesthesiol Scand 2003;47:958–967. [PubMed: 12904187]

Manole MD, Hickey RW, Momoi N, Tobita K, Tinney JP, Suciu GP, Johnnides MJ, Clark RS, Keller BB. Preterminal gasping during hypoxic cardiac arrest increases cardiac function in immature rats. Pediatr Res 2006;60:174–179. [PubMed: 16864699]

Michenfelder JD, Milde JH. Postischemic canine cerebral blood flow appears to be determined by cerebral metabolic needs. J Cereb Blood Flow Metab 1990;10:71–76. [PubMed: 2298838]

Mortberg E, Cumming P, Wiklund L, Wall A, Rubertsson S. A PET study of regional cerebral blood flow after experimental cardiopulmonary resuscitation. Resuscitation 2007;75:98–104. [PubMed: 17499906]

Mujsce DJ, Christensen MA, Vannucci RC. Cerebral blood flow and edema in perinatal hypoxic-ischemic brain damage. Pediatr Res 1990;27:450–453. [PubMed: 2345670]

Nehlig A, de Vasconcelos A Pereira, Boyet S. Postnatal changes in local cerebral blood flow measured by the quantitative autoradiographic [14C]iodoantipyrine technique in freely moving rats. J Cereb Blood Flow Metab 1989;9:579–588. [PubMed: 2777930]

Neubauer JA, Edelman NH. Nonuniform brain blood flow response to hypoxia in unanesthetized cats. J Appl Physiol 1984;57:1803–1808. [PubMed: 6439706]

Nishizawa H, Kudoh I. Cerebral autoregulation is impaired in patients resuscitated after cardiac arrest. Acta Anaesthesiol Scand 1996;40:1149–1153. [PubMed: 8933858]

Qiao M, Latta P, Foniok T, Buist R, Meng S, Tomanek B, Tuor UI. Cerebral blood flow response to a hypoxic-ischemic insult differs in neonatal and juvenile rats. Magma 2004;17:117–124. [PubMed: 15538659]

Rosenberg AA. Cerebral blood flow and O2 metabolism after asphyxia in neonatal lambs. Pediatr Res 1986;20:778–782. [PubMed: 3737291]

Safar P, Xiao F, Radovsky A, Tanigawa K, Ebmeyer U, Bircher N, Alexander H, Stezoski SW. Improved cerebral resuscitation from cardiac arrest in dogs with mild hypothermia plus blood flow promotion. Stroke 1996;27:105–113. [PubMed: 8553385]

Schleien CL, Koehler RC, Shaffner DH, Eberle B, Traystman RJ. Blood-brain barrier disruption after cardiopulmonary resuscitation in immature swine. Stroke 1991;22:477–483. [PubMed: 1902598]

Singh NC, Kochanek PM, Schiding JK, Melick JA, Nemoto EM. Uncoupled cerebral blood flow and metabolism after severe global ischemia in rats. J Cereb Blood Flow Metab 1992;12:802–808. [PubMed: 1506444]

Snyder JV, Nemoto EM, Carroll RG, Safar P. Global ischemia in dogs: intracranial pressures, brain blood flow and metabolism. Stroke 1975;6:21–27. [PubMed: 1111179]

Statler KD, Kochanek PM, Dixon CE, Alexander HL, Warner DS, Clark RS, Wisniewski SR, Graham SH, Jenkins LW, Marion DW, Safar PJ. Isoflurane improves long-term neurologic outcome versus fentanyl after traumatic brain injury in rats. J Neurotrauma 2000;17:1179–1189. [PubMed: 11186231]

Sterz F, Leonov Y, Safar P, Johnson D, Oku K, Tisherman SA, Latchaw R, Obrist W, Stezoski SW, Hecht S, et al. Multifocal cerebral blood flow by Xe-CT and global cerebral metabolism after prolonged cardiac arrest in dogs. Reperfusion with open-chest CPR or cardiopulmonary bypass. Resuscitation 1992;24:27–47. [PubMed: 1332160]

Sundgreen C, Larsen FS, Herzog TM, Knudsen GM, Boesgaard S, Aldershvile J. Autoregulation of cerebral blood flow in patients resuscitated from cardiac arrest. Stroke 2001;32:128–132. [PubMed: 11136927]

Ten VS, Pinsky DJ. Endothelial response to hypoxia: physiologic adaptation and pathologic dysfunction. Curr Opin Crit Care 2002;8:242–250. [PubMed: 12386504]

Wainwright MS, Grundhoefer D, Sharma S, Black SM. A nitric oxide donor reduces brain injury and enhances recovery of cerebral blood flow after hypoxia-ischemia in the newborn rat. Neurosci Lett 2007;415:124–129. [PubMed: 17270345]

Young KD, Gausche-Hill M, McClung CD, Lewis RJ. A prospective, population-based study of the epidemiology and outcome of out-of-hospital pediatric cardiopulmonary arrest. Pediatrics 2004;114:157–164. [PubMed: 15231922]

Zhang W, Williams DS, Koretsky AP. Measurement of rat brain perfusion by NMR using spin labeling of arterial water: in vivo determination of the degree of spin labeling. Magn Reson Med 1993;29:416–421. [PubMed: 8383791]

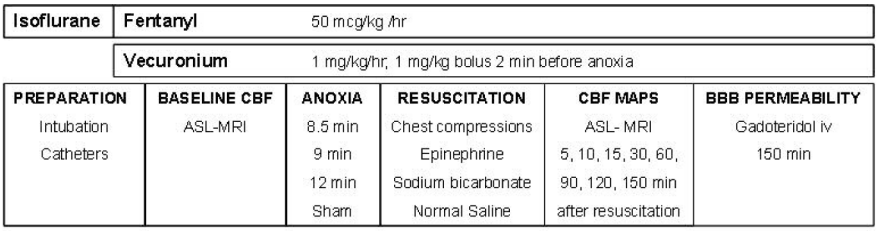

Figure 1.
Graphic representation of the methods.

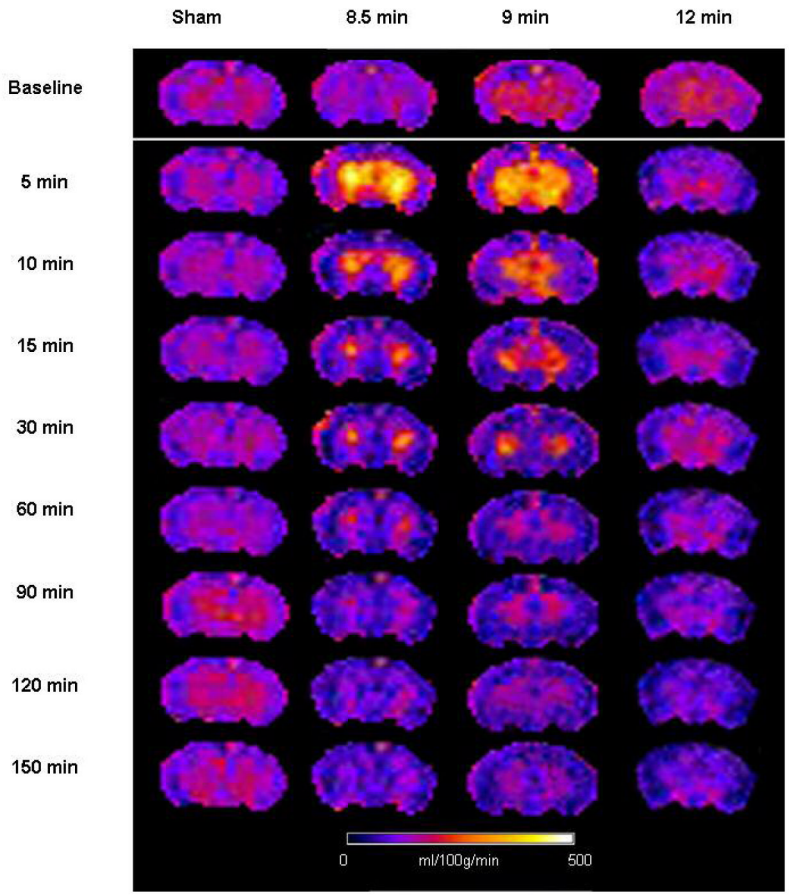

Figure 2.
Cerebral blood flow maps for one representative animal in each group. Notice early hyperemia after 8.5 and 9 min asphyxia and hypoperfusion with absence of early hyperemia after 12 min asphyxia.

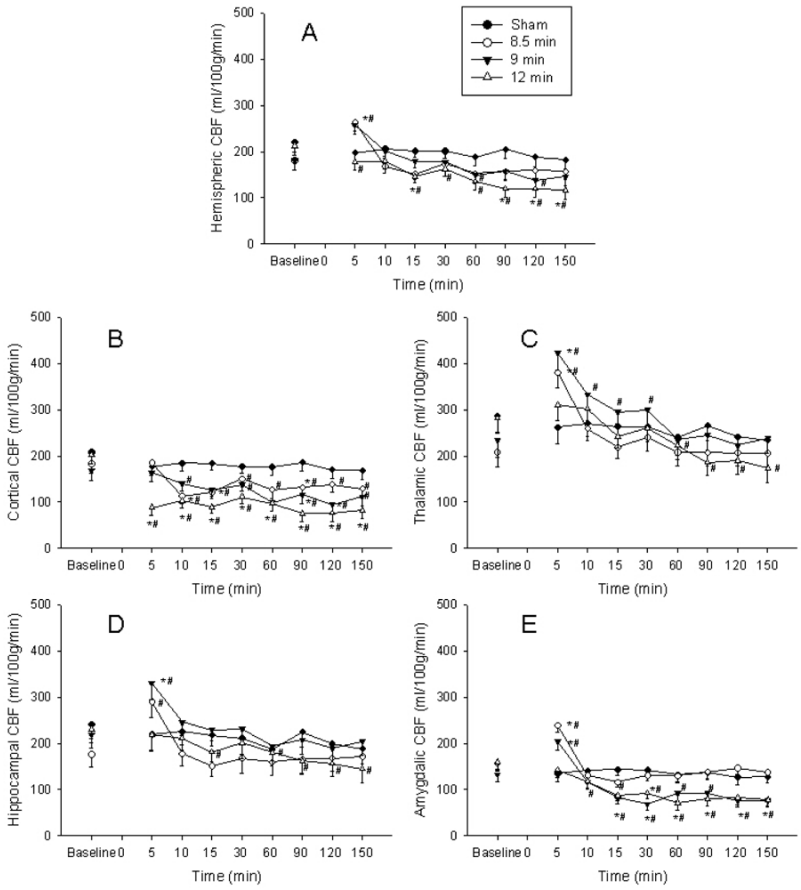

Figure 3.

Global hemispheric and regional cerebral blood flow (CBF) at baseline and after return of spontaneous circulation (ROSC). Time zero represents time of ROSC for the asphyxia groups. A. Hemispheric CBF. Early hyperemia is present in the 8.5 and 9 min groups and absent in the 12 min group. Hypoperfusion is present in the 12 min group and at few time points in the 9 min group. B. Cortical CBF. Early hyperemia is absent in the cortex. Hypoperfusion is immediate in the 12 min group and later in the 8.5 and 9 min groups. C. Thalamic CBF. Early hyperemia is seen in the 8.5 and 9 min groups. Hypoperfusion is seen in the 12 min group only. D. Hippocampal CBF. Early hyperemia is seen in the 8.5 and 9 min groups only. Hypoperfusion is seen in the 12 min group. E. Amygdalic CBF. Early hyperemia is seen in the 8.5 and 9 min groups. Hypoperfusion is early in the 12 min group and delayed in the 9 min group. Error bars represent standard error of the mean. * $p<0.05$ vs. sham, # $p<0.05$ vs. baseline.

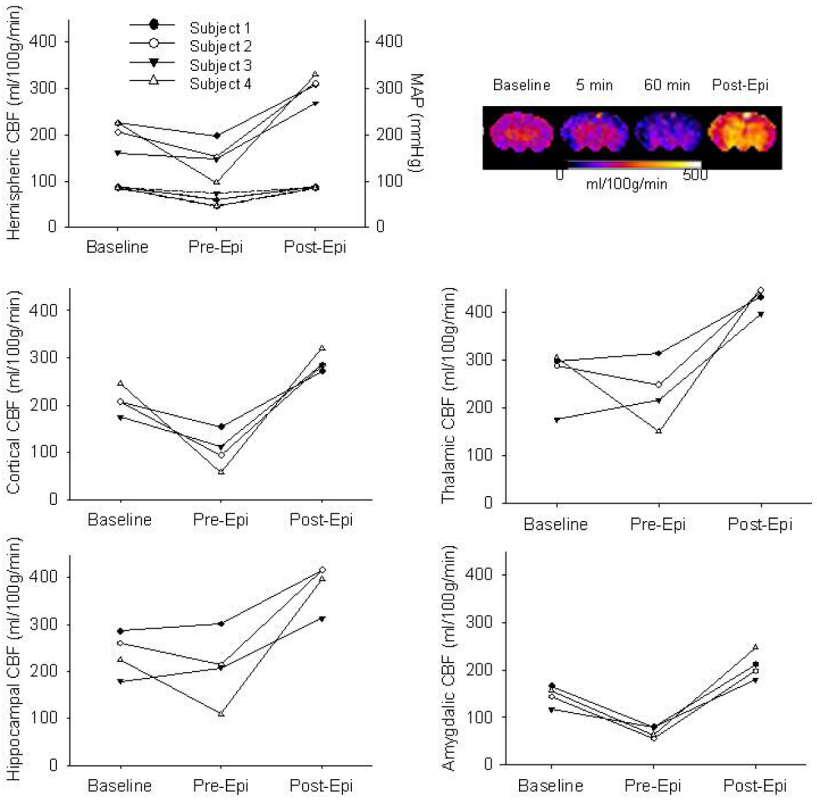

Figure 4.

Relationship between mean arterial pressure (MAP) and cerebral blood flow (CBF). CBF and MAP at baseline and after cardiac arrest, before infusion of epinephrine (Pre-Epi) and after infusion of epinephrine (Post-Epi). CBF color map for one representative animal at baseline and after cardiac arrest, before (1h) and after epinephrine infusion. Upper portion of the hemispheric CBF graph represents CBF, whereas the lower portion represents MAP for each subject.

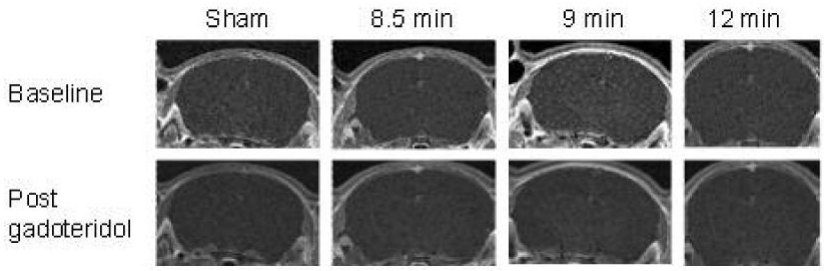

Figure 5.
Blood Brain Barrier Function after CA. There is no difference in the signal obtained before and after administration of gadoteridol, in all groups studied.

Table 1

Baseline Weight, time to cardiac arrest (CA) and duration of CA for the four groups of rats.

	Sham n=6	**8.5 min n=7**	**9 min n=6**	**12 min n=7**
Weight	36.5±0.9	35.4±1.7	35.3±0.9	37±1.1
Time to CA (min)	n/a	3±0.4	3±0.3	2.7±0.2
Duration of CA (min)	n/a	5.3±0.4*	6±0.3*	9.1±0.2*

Data are represented as mean±SEM.

*$p<0.05$

Table 2

Physiological variables at baseline and after resuscitation in the four groups of rats. Mean arterial pressure (MAP).

		Baseline	5 min	15 min	90 min	150 min
MAP	Sham	77±5	75±5	75±5	70± 5	74±6
	8.5 min	66±5	90±5 †	55±5 †*	52±5 †*	58±5 †
	9 min	81±5	86±5	55±5 †*	49±5 †*	56±5 †*
	12 min	85±5	72±5 †	64±5 †	61±5 †*	53±5 †*
$PaCO_2$	Sham	38±6	n/a	44±20	37±13	43±7
	8.5 min	36±6	n/a	44±8	43±3	55±8 †*
	9 min	36±6	n/a	41±11	46±8 †	51±11 †
	12 min	34±5	n/a	48±21	34±15	34±15
PaO_2	Sham	190±10	n/a	245±30	171±6	153±11
	8.5 min	220±28	n/a	226±11	204±31	196±23
	9 min	194±15	n/a	242±17	158±31	140±10
	12 min	173±24	n/a	106±25 *	175±36	170±43
pH	Sham	7.23±0.01	n/a	7.19±0.01	7.17±0.02	7.14±0.01
	8.5 min	7.28±0.01	n/a	7.27±0.09	7.35±0.04 *	7.33±0.02 *
	9 min	7.26±0.05	n/a	7.19±0.03	7.24±0.02	7.26±0.03 *
	12 min	7.24±0.02	n/a	7.07±0.05 †	7.24±0.04	7.28±0.03 *

Data are represented as mean±SEM.

* $p<0.05$ vs. sham

† $p<0.05$ vs. baseline.